Role of short-range and tensor correlations in nuclei

Journal of Physics: Conference Series **312** (2011) 022007 doi:10.1088/1742-6596/312/2/022007

Role of short-range and tensor correlations in nuclei

A Rios[1], W H Dickhoff[2] and A Polls[3]

[1]Department of Physics, Faculty of Engineering and Physical Sciences, University of Surrey, Guildford, Surrey GU2 7XH, United Kingdom
[2]Department of Physics, Washington University, St. Louis, Missouri 63130, USA
[3]Departament d'Estructura i Constituents de la Matèria and Institut de Ciències del Cosmos, Universitat de Barcelona, Avda. Diagonal 647, E-08028 Barcelona, Spain

E-mail: a.rios@surrey.ac.uk

Abstract. The present theoretical understanding of the role of short-range correlations in nuclei near stability is reviewed. Two effects are identified in particular: first, the depletion of mean-field single-particle strength that is no longer available to participate in low-lying excitations. Second, the admixture of high-momentum nucleons in the ground state that is implied by the vanishing relative wave functions of pairs in the medium. The role of the tensor force will be further clarified by discussing isospin-polarized matter. It is demonstrated that the depletion of the proton and neutron Fermi seas depends strongly on the nuclear tensor force and appears to be determined by nucleon-nucleon scattering data. The increased role of short-range and tensor correlations for the minority species makes the case for further experimental scrutiny of nuclei with large neutron excess. Appropriate data of single- and two-nucleon knockout experiments are employed to illustrate the role of short-range and tensor correlations.

1. Introduction

The nucleon-nucleon (NN) interaction is extremely repulsive at short distances [1]. As a consequence of this strong repulsion, the probability of finding two nucleons close to each other is substantially suppressed. In turn, such a decrease in the configuration space components implies the population of high-momentum components in the many-body wave function of nuclear systems. These significant modifications, induced by the NN interaction, cannot be described within an independent particle model and are generically referred to as *correlations* [2]. An additional mechanism that provides high-momentum components is associated with the NN tensor force, which is, among other things, required to obtain the correct quadrupole moment of the deuteron [1]. The partial-wave mixing due to the tensor force is responsible for strong correlation effects. Fully non-perturbative nuclear many-body calculations, which are able to deal with the sizable effect associated to short-range (SRC) and tensor correlations (TC), are needed to understand the properties of nuclear systems from an *ab-initio* perspective. While there is some freedom in the parametrization of the short distance behaviour of the NN interaction, there is now evidence from lattice QCD calculations that the features of a strong repulsive short-range core emerge from first principles [3]. This repulsive component is also required by the experimental NN phase shift analysis and is incorporated in one way or another in all realistic NN interactions. By obtaining results based on different potentials, one can get a qualitative measure of the uncertainty associated to the role of short-range and tensor correlations in nuclei. Here we shall focus on the relatively soft CDBonn interaction [4] and

the harder Argonne V18 (Av18) force [5], as two canonical examples of high-quality fits to NN scattering data.

Recent experiments at Jefferson Laboratory have clarified several aspects of the role of SRC and TC in determining the properties of nucleons in the nuclear medium. An unambiguous signature of the presence of high-momentum nucleons was identified in an $(e, e'p)$ experiment on ^{12}C [6]. In the domain of missing energy and momentum probed by the experiment, the amount of single-particle strength identified corresponded reasonably to scaled theoretical predictions of the self-consistent Green's function (SCGF) calculation for ^{16}O [7] and correlated basis functions calculations for nuclear matter in the local density approximation [8]. In even more demanding exclusive two-nucleon knock-out experiments on ^{16}O to the ground state of ^{14}C [9, 10], direct evidence for the presence of short-range proton-proton (pp) correlations was identified, in reasonable agreement with theoretical calculations [11, 12]. Definitive evidence for the importance of the nuclear tensor force in generating high-momentum components was presented in Ref. [13], where the ratio of knocked-out proton-neutron (pn) to pp pairs from ^{12}C was found to be around 20. Theoretical relative momentum distributions exhibit a similar enhancement of pn over pp correlations due to the tensor force in the domain of momenta probed in this Jefferson Lab experiment [14].

2. Depletion of symmetric nuclear systems

Particle number conservation requires the high-momentum components to be accompanied by a corresponding depletion of the population of states within the nuclear Fermi sea [15]. A distinctive feature of this depletion in nuclear matter is its essentially momentum-independent character, except in the immediate vicinity of the Fermi surface [16]. For all realistic NN interactions, different many-body techniques consistently predict a depletion of the nuclear Fermi sea of a little over 15%, of which around a third is caused by tensor correlations. An $(e, e'p)$ experiment on ^{208}Pb at NIKHEF in a large domain of missing energy and a momentum range corresponding to the mean-field Fermi sea confirmed that a global depletion between 15 and 20% of proton orbits below the Fermi energy explains all the measured coincidence cross sections [17, 18]. The differences with respect to nuclear matter calculations can be largely attributed to long-range correlations [19]. Let us note that the depletion of liquid ^{3}He for very small momenta is considerably larger and reaches about 50% [20], while the depletion of the electron Fermi sea in closed-shell atoms is essentially zero [21].

A particularly well-suited technique to study the depletion of nuclear systems is the SCGF method [2]. Within this approach correlations are accounted for by a fully self-consistent treatment of ladder diagrams for the interaction between particles that propagate with respect to a correlated (by short-range and tensor effects) ground state. The infinite sum of particle-particle and hole-hole diagrams is effectively included in the in-medium T-matrix, which fulfills a Lippmann-Schwinger-like equation:

$$\begin{aligned}\langle \boldsymbol{k}_1\boldsymbol{k}_2|T(\Omega_+)|\boldsymbol{k}_3\boldsymbol{k}_4\rangle_A &= \langle \boldsymbol{k}_1\boldsymbol{k}_2|V|\boldsymbol{k}_3\boldsymbol{k}_4\rangle_A \\ &+ \sum_{\boldsymbol{k}_5,\boldsymbol{k}_6} \langle \boldsymbol{k}_1\boldsymbol{k}_2|V|\boldsymbol{k}_5\boldsymbol{k}_6\rangle_A \, \mathcal{G}^0_{II}(k_5,k_6;\Omega_+) \, \langle \boldsymbol{k}_5\boldsymbol{k}_6|T(\Omega_+)|\boldsymbol{k}_3\boldsymbol{k}_4\rangle_A \, . \end{aligned} \quad (1)$$

Here, we have introduced the NN potential (properly antisymmetrized) and spin and isospin indices have been omitted for simplicity. The retarded $\mathcal{G}^0_{II}$ is obtained from the product of two spectral functions and a phase space factor describing the intermediate propagation of particle-particle and hole-hole pairs

$$\mathcal{G}^0_{II}(k,k';\Omega_+) = \int_{-\infty}^{\infty} \frac{\mathrm{d}\omega}{2\pi}\frac{\mathrm{d}\omega'}{2\pi} \mathcal{A}(k,\omega)\mathcal{A}(k',\omega') \frac{1-f(\omega)-f(\omega')}{\Omega_+ - \omega - \omega'} \, , \quad (2)$$

properly accounting for Pauli blocking effects. For practical purposes, the solution of the self-consistent problem is performed at finite temperature, T, in which case the occupation factors, $f(\omega) = \left[1 + e^{(\omega-\mu)/T}\right]^{-1}$, are Fermi-Dirac distributions [2]. In general terms, the retarded self-energy fulfills the dispersion relation

$$\mathrm{Re}\Sigma_{\mathcal{R}}(k,\omega) = \Sigma_{HF}(k) - \mathcal{P}\int_{-\infty}^{\infty} \frac{\mathrm{d}\omega'}{\pi} \frac{\mathrm{Im}\Sigma_{\mathcal{R}}(k,\omega')}{\omega - \omega'} \,. \tag{3}$$

The first term in this expression corresponds to an energy-independent Hartree-Fock contribution

$$\Sigma_{HF}(k) = \sum_{\boldsymbol{k'}} \left\langle \boldsymbol{k}\boldsymbol{k'}|V|\boldsymbol{k}\boldsymbol{k'}\right\rangle_A n(k') \,, \tag{4}$$

where $n(k)$ is the momentum distribution. The latter includes correlation effects and is computed from the spectral function

$$n(k) = \nu \int_{-\infty}^{\infty} \frac{\mathrm{d}\omega}{2\pi} \mathcal{A}(k,\omega) f(\omega) \,, \tag{5}$$

where $\nu = 4$ ($\nu = 2$) accounts for the spin-isospin degeneracy of nuclear (neutron) matter. The energy-dependent, dispersive contribution to the self-energy describes many-body processes that go beyond the basic mean-field approximation. The imaginary part of the retarded self-energy in the ladder approximation reads

$$\mathrm{Im}\Sigma_{\mathcal{R}}(k,\omega) = \sum_{k'} \int_{-\infty}^{\infty} \frac{\mathrm{d}\omega'}{2\pi} \left[f(\omega') + b(\omega+\omega')\right] \mathcal{A}(k',\omega') \left\langle \boldsymbol{k}\boldsymbol{k'}|\mathrm{Im}T(\omega+\omega'_+)|\boldsymbol{k}\boldsymbol{k'}\right\rangle \,, \tag{6}$$

and is given in terms of the in-medium interaction, the spectral function and phase space factors, including a Bose-Einstein distribution, $b(\Omega) = \left[e^{-(\Omega-2\mu)/T} - 1\right]^{-1}$. Once the real and imaginary parts of the self-energy are computed, one can feed back this information into the spectral function via the Dyson equation

$$\mathcal{A}(k,\omega) = \frac{-2\mathrm{Im}\Sigma_{\mathcal{R}}(k,\omega)}{\left[\omega - \frac{k^2}{2m} - \mathrm{Re}\Sigma_{\mathcal{R}}(k,\omega)\right]^2 + \left[\mathrm{Im}\Sigma_{\mathcal{R}}(k,\omega)\right]^2} \,, \tag{7}$$

which can in turn be used to compute a new $\mathcal{G}^0_{II}$. By iterating this procedure until convergence, the SCGF result within the ladder approximation is obtained and one has access to the spectral functions of a nuclear system at a given density and temperature. In addition to the single-particle properties, the spectral function also determines the thermodynamical properties, like the total energy via the Galitskii-Migdal-Koltun sum rule [22] as well as the entropy within the Luttinger-Ward formalism [23]. Self-consistency represents a democratic treatment of all the particles considered in the problem: the one for which the self-energy is calculated, as well as the ones it interacts with. Its importance stems from the fact that sum rules are preserved [24] and also that thermodynamical consistency is fulfilled [23].

Recently, numerical calculations including full off-shell effects have become available at finite temperature [23, 25]. Thermal effects are expected to smooth out the momentum distribution near the Fermi momentum, but they hardly affect the small and very high-momentum content of the ground state. Interaction-induced correlations have a distinctive signature in the momentum distribution, removing strength at momenta below the Fermi surface and shifting it to high momenta. As a matter of fact, thermal correlations produce a similar signature on the momentum distribution: low momenta are depopulated, while high momenta are occupied. The

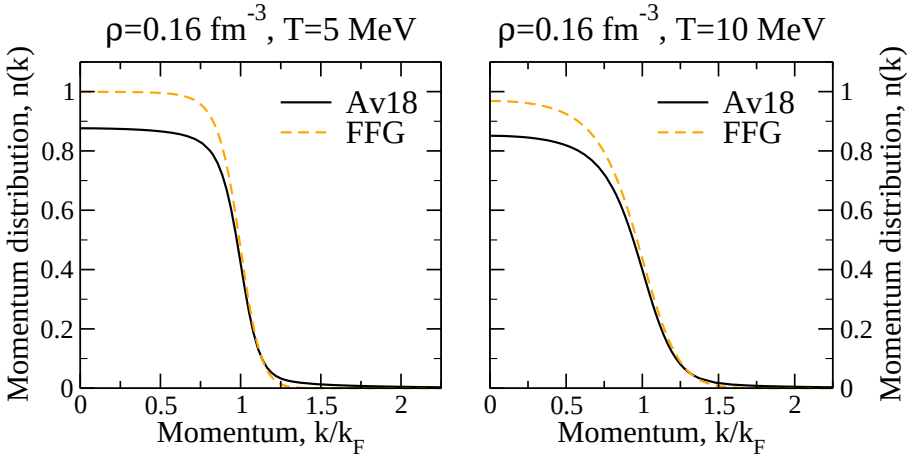

Figure 1. Correlated momentum distribution obtained with the Av18 interaction at $\rho = 0.16$ fm^{-3} and two temperatures: $T = 5$ MeV (left panel) and $T = 10$ MeV (right panel). The dashed line corresponds to the momentum distribution of the Free Fermi Gas under the same conditions.

amount of low-momentum depletion and high-momentum population, however, is significantly different for both types of correlations. One can distinguish between them by comparing the fully correlated SCGF prediction with the Free Fermi Gas (FFG) results, which are only sensitive to thermal correlations [26]. To this end, in Fig. 1 we show the momentum distribution, $n(k)$, of symmetric nuclear matter (SNM) for Av18 and for the FFG at $\rho = 0.16$ fm^{-3} and $T = 5$ MeV (left panel) and 10 MeV (right panel). At the lower temperature, the Fermi-Dirac distribution of the FFG deviates very little from a step function, $\Theta(k_F - k)$, which describes the $n(k)$ of the FFG at zero temperature. One can conclude that the thermal effects are small in the deep interior of the Fermi sea in these conditions, while they modulate $n(k)$ close to the Fermi surface. For the correlated case, $n(k)$ is rather flat below k_F and it presents a sizable depletion, mainly caused by dynamical NN correlations. At a larger temperature (right panel), thermal effects do not only modify the FFG $n(k)$ around the Fermi surface, but they also produce a depletion deep inside the Fermi sea. The lowest momentum state is depopulated by a few percent, $n(0) = 0.97$. The shape of $n(k)$ differs significantly from the step function, due to the loss of degeneracy. At this temperature, the momentum distribution of the correlated system deep inside the Fermi sea exhibits a depletion, $1 - n(0) = 15\%$, which is approximately the sum of the depletion associated with the dynamic NN correlations ($\sim 13\%$) plus the one coming from the thermal distribution of the FFG (3%).

Consequently, the depletion of the momentum distribution below the Fermi surface can be taken as a measure of both thermal and dynamical correlations in many-body systems. In the degenerate regime, where thermal effects are unimportant, the amount of strength removed at low momenta is closely related to the structure of the underlying NN force. For high temperatures or low densities, $n(k)$ is softened by thermal correlations. Figure 2 displays the density dependence of the occupation of this state for SNM (left panel) and pure neutron matter (PNM) (right panel). Results for the Av18 (CDBonn) interaction are shown in solid (dotted) lines, while dashed lines represent the FFG depletion under the same conditions. The non-interacting depletion is necessary to disentangle the influence of thermal correlations on the low-momentum components. At high densities, degeneracy dominates over temperature, and $n(0) = 1$ as expected from the zero temperature FFG momentum distribution. This degenerate regime determines the region where SRC and TC dominate the depletion and therefore can be

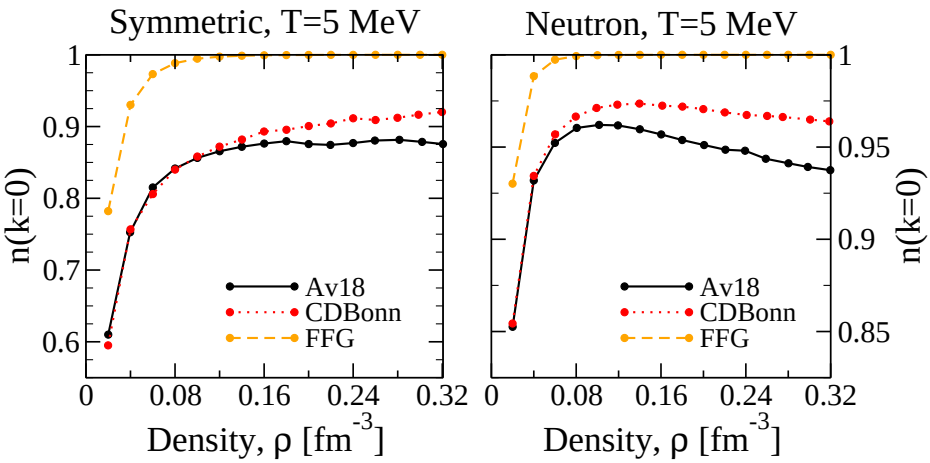

Figure 2. Density dependence of the occupation of the lowest momentum state at $T = 5$ MeV for Av18 (solid lines), CDBonn (dotted lines) and the FFG (dashed lines). The left (right) panel corresponds to nuclear (neutron) matter results. Note the different vertical scales.

taken as faithful representatives of zero-temperature calculations. At lower densities, however, the FFG drops rapidly as density decreases, indicating that thermal effects dominate the low-momentum components of $n(k)$. The decrease observed in $n(0)$ for the correlated case should therefore be associated with temperature effects rather than with NN correlations.

If we take the deviation of $n(0)$ from 1 as a measure of correlations, we can say that PNM is "less correlated", in general, than SNM (note the different vertical scale of the two panels of Fig. 2). Moreover, the behavior of $n(0)$ as a function of density in the region where thermal effects are unimportant is very different for PNM and SNM. In neutron matter, as the density increases, the population of low momenta drops. This result agrees with the intuitive idea that, as particles are closer together on average, the effect of the short-range core increases and low-momentum strength is shifted to high momenta. Also in accordance with this picture, the depletion is more important for an interaction with a harder core (Av18) than for a softer force (CDBonn) [27]. In stark contrast, for SNM the opposite density dependence is observed: the depletion is constant or *decreases* as the density increases. For Av18, the depletion saturates at a constant value of $n(0) \sim 0.87$ as density increases, while for CDBonn a clear increase of $n(0)$ with density is observed.

What causes such a different behavior in the density dependence of $n(0)$? The major difference between neutron and nuclear matter lies in the role of the strong ${}^3S_1 - {}^3D_1$ tensor component, which is only active in the latter. The effect of this component is twofold. On the one hand, it increases the depletion as compared to the effect of SRC by themselves, as seen by comparing SNM and PNM results. On the other hand, tensor components seemingly modify the density dependence of $n(0)$. In Ref. [26], we have analyzed the origin of these effects. We have concluded that the anomalous density dependence is tightly connected to the strong binding effects associated to the tensor force.

3. Correlations in asymmetric nuclear matter

So far, we have discussed uniform nuclear systems with a single species: the nucleon, in the case of SNM, and the neutron, in the case of PNM. For a fixed total density, one can switch from one system to the other by modifying the relative concentration of neutrons and protons, defined by

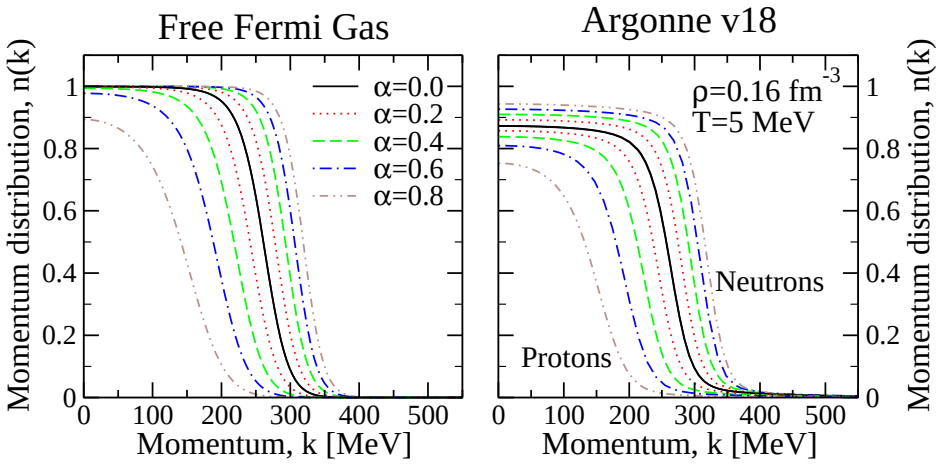

Figure 3. Isospin asymmetry dependence of the Free Fermi gas (left panel) and the correlated momentum distribution from Av18 (right panel). The density ($\rho = 0.16$ fm^{-3}) and temperature ($T = 5$ MeV) are fixed and the results for different asymmetries are shown in different line-styles.

the asymmetry parameter

$$\alpha = \frac{\rho_n - \rho_p}{\rho_n + \rho_p} \,. \tag{8}$$

The SCGF method within the ladder approximation can be generalized to the case of asymmetric nuclear matter and partially isospin-polarized systems can thus be analyzed [28, 29]. Since the approach accounts for both the SRC and TC associated with the underlying NN interaction, it can be used to generate quantitative predictions for the importance of different types of correlations in isospin asymmetric systems.

The study of the asymmetry dependence of SRC and TC is motivated to a large extent by the (future) study of rare isotopes with large neutron excess. Experimental studies employing heavy-ion knock-out reactions already suggest that the removal probability for the minority species is strongly reduced compared to shell-model calculations, whereas the majority species exhibits properties that are essentially mean-field like [30]. Smaller effects have been obtained from the analysis of transfer reactions [31] and microscopic *ab initio* calculations [32]. These differences should be clarified to allow an unambiguous extraction of these properties for rare isotopes [33]. Similar tendencies have been obtained for the spectroscopic factors of protons from a combined dispersive optical model analysis of a sequence of Ca isotopes [34, 35]. Fitting a huge collection of elastic proton scattering data while including results obtained from $(e, e'p)$ reactions for quantities below the Fermi energy, the emerging complex optical potentials for protons exhibit a striking increase in surface absorption with increasing nucleon asymmetry. This translates into a qualitatively similar tendency in spectroscopic factors as obtained from the zero-momentum occupation of protons calculated in the bulk for isospin-polarized nuclear matter [29]. We note that the dispersive optical model analysis has not yet been sensitive to an asymmetry dependence in the volume potentials which are most closely associated with infinite matter results. The analysis of nuclei with larger nucleon asymmetry may clarify this issue in the future.

The asymmetry dependence of the neutron and proton momentum distribution is presented in Fig. 3 at $\rho = 0.16$ fm^{-3} and $T = 5$ MeV. The left (right) panel contains the results for FFG (Av18). For $\alpha = 0$ (symmetric case), the momentum distributions of neutrons and protons

coincide in both cases. Let us discuss first the left panel. For $\alpha = 0$, the thermal effects on $n(k)$ are only visible at the Fermi surface and almost no depletion occurs inside the Fermi sea. The same is true for the most abundant component as asymmetry increases: the depletion is negligible and the Fermi momentum is displaced to larger values. For protons, however, $n(k)$ is clearly affected by temperature, exhibiting a large change in shape in a wide region of momenta. At large asymmetries, in particular, the momentum distribution of the less abundant components differs substantially from the step function, decreasing the occupation at the origin. When increasing the asymmetry, the less abundant component moves closer to a classical momentum distribution, while the most abundant component becomes more degenerate. This analysis suggests that one should take into account thermal corrections when analyzing the change in asymmetry of $n_\tau(k)$ also for the correlated case.

Focusing on the right panel, one observes that the most abundant component (neutrons for positive α) gets less depleted when the asymmetry increases, *i.e.* neutrons become "less correlated". This is in contrast to the FFG results, which, for neutrons, exhibit no change inside the Fermi sea. The decrease of depletion for the most abundant component in this density and temperature should therefore be taken as a pure NN correlation effect. This behavior can be explained in simple terms as follows. Although the total number of pairs is the same when increasing the asymmetry at constant density, some of the pn pairs are replaced by neutron-neutron pairs. The latter correlations are weaker than the pn ones, due to the absence of tensor effects, and therefore neutrons become less correlated at large α's. Conversely, the momentum distributions of the less abundant species (protons) become more depleted with asymmetry. A single proton sees an increasing number of neutrons when the asymmetry increases, *i.e.* pp pairs are replaced by the more correlated pn pairs, which results into a more depleted proton momentum distributions. Together with this, protons "feel" more the effect of temperature. At finite temperature, $n_p(k)$ becomes dominated by thermal effects at large asymmetries. The plateau associated with particle states, for instance, which is clearly observed for neutrons at all asymmetries, gets washed out for protons at large α. Consequently, one should be careful in associating the increase of the depletion of protons only to dynamical NN correlation, because the momentum distribution of the less abundant component can be strongly influenced by thermal effects.

The information about the isospin dependence of the depletion is summarized in the left panel of Fig. 4, where $n_\tau(0)$ is plotted as a function of the asymmetry at $T = 5$ MeV for $\rho = 0.16$ fm^{-3} and several NN interactions. The FFG (dashed lines) results are compared to those obtained with a wide range of NN interactions. Again, the FFG results provide a measure of thermal effects. On the one hand, the occupation of the most abundant component at zero momentum does not change when the asymmetry increases, indicating that this species is totally degenerate in the whole range of asymmetries. On the other hand, the corresponding occupation of protons (the less abundant component) is close to 1 at small asymmetries and decreases as the asymmetry increases. As a matter of fact, in the limit $\alpha \to 1$, the protons become an impurity gas in a Fermi sea of neutrons, thus behaving as a classical gas with $n_p(0) \to 0$. The steepness of the change in $n_p(0)$ depends on the total density and the temperature of the system. At a higher density, the thermal effects affecting protons would not set in unless the asymmetry was very large [15]. Let us stress the idea that this is a pure thermal effect: for the FFG at zero temperature, $n_\tau(0) = 1$ for both protons and neutrons at all asymmetries.

For the correlated depletion, the occupation of the zero momentum state is an increasing (decreasing) function of the asymmetry for the more (less) abundant component. The behavior is very similar for all NN interactions, although the occupations for Av18 are systematically smaller than those for CDBonn. The comparison with the FFG allows us to identify the regime in which NN correlations dominate over thermal effects. At $T = 5$ MeV and $\rho = 0.16$ fm^{-3}, for instance, and up to asymmetries of about $\alpha \sim 0.4 - 0.6$, the occupations of neutrons and

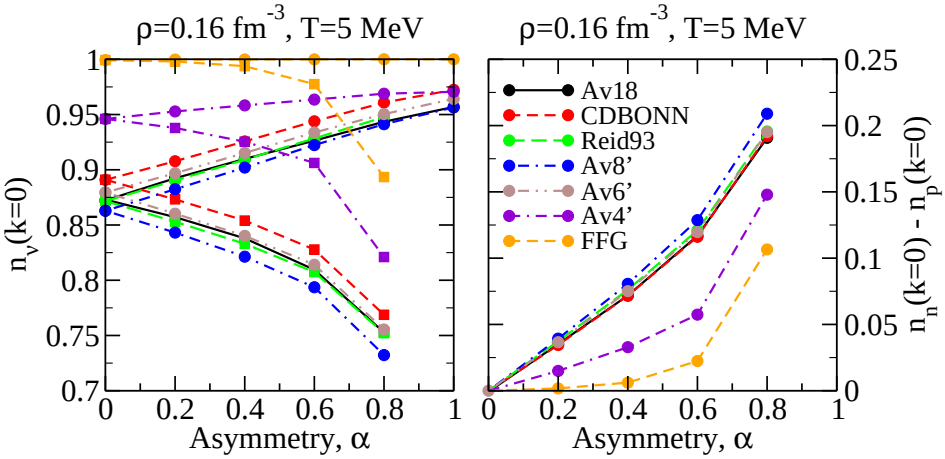

Figure 4. Left panel: isospin asymmetry dependence of the occupation of the lowest momentum state, for a total fixed density of $\rho = 0.16$ fm^{-3} and $T = 5$ MeV. Neutron (proton) occupations are shown with circles (squares). Results for different NN potentials are shown in different line-styles. Right panel: difference of the neutron and proton occupation of the lowest momentum state as a function of isospin asymmetry for different NN potentials in the same conditions.

protons can be attributed to dynamical correlations and should provide a good estimate for the case of zero temperature. Up to these asymmetries, both the neutron and the proton depletion change almost linearly with asymmetry. In the right panel, the depletion of protons starts to bend down for larger asymmetries, due to the onset of thermal effects. In a more degenerate case (right panel), where thermal effects are almost negligible, the asymmetry dependence of both $n_\tau(0)$'s is again found to be linear.

Asymmetries of stable nuclei belong to the lower range of asymmetries, *i.e.* $\alpha \sim 0.2$ for ^{208}Pb. The SCGF predictions should be valid in this range, where thermal effects are unimportant. Unfortunately, the difference between the occupation of protons at this asymmetry and the symmetric case is only $\sim 2\%$, too small to allow experimental verification. Nuclei at larger asymmetry produced at future rare isotope facilities may provide a better testing ground. Moreover, integrated effects over the whole neutron and proton density profiles might also enhance the effect of asymmetry. Let us note that, for finite nuclei, one should also take into account surface properties and their isospin dependence. In particular, an asymmetry dependent effect associated with surface properties has been identified for protons in Ca isotopes [34, 35].

A surprising feature arises when comparing the different NN interaction results in the left panel of Fig. 4. In spite of the differences observed in both SNM and PNM for the Av18 and CDBonn results, the asymmetry dependence of $n_\tau(0)$ is very similar for both interactions. This is shocking because, as we have stressed so far, both forces have a rather different short-range behavior and tensor structure. Given the almost linear dependence of $n_\tau(0)$ with asymmetry, a better insight into these differences can be gained by plotting the difference $n_n(0) - n_p(0)$. In the right panel of Fig. 4, we present this "iso-depletion" for different interactions as a function of the asymmetry at $T = 5$ MeV and $\rho = 0.16$ fm^{-3}. The right panel shows that this difference is the same for a wide variety of modern NN potentials, independently of their short-range or operatorial structure. This suggests that the iso-depletion is fixed by the phase-shifts, most probably via their isospin dependence.

In the right panel, there are two results that fall below the main iso-depletion line. Immediately below most of the interactions, one finds the results corresponding to the Av4'

potential. This has an extremely simplified operatorial structure, with only a spin-isospin part and no tensor components, and is fitted to reproduce the binding energy of the deuteron [36]. The fact that it lies significantly below the other results shows the importance of TC for isospin asymmetric systems. It appears that the tensor force increases the difference between neutron and proton momentum distributions as asymmetry increases. Let us again stress the fact that such an agreement for different potentials is very surprising, particularly if one considers the fact that the momentum distributions of neutrons and protons can be different for each potential.

The FFG iso-depletion is, in all the cases explored, also below the correlated results. This highlights the importance of NN interaction-induced effects in $n(k)$. Let us stress that the effect of beyond mean-field correlations is essential in this case. Mean-field calculations, either with realistic or phenomenological forces, will predict results of the same order of magnitude of the FFG. Again, the latter only provides a measure of what we have called thermal effects. For instance, the correlated iso-depletion at the largest asymmetry considered here should be significantly affected by thermal effects and therefore one should not take that value as a NN dynamical correlation effect.

4. Conclusions

The aim of the present contribution is to provide a better understanding of the effect of short-range and tensor correlations in nuclei, as a function of density, temperature and isospin asymmetry, for different choices of realistic interactions. The SCGF method, when implemented at the level of ladder diagrams, is capable of providing answers to these questions. We have studied both one-component systems (symmetric matter and pure neutron matter) as a function of density, as well as isospin-polarized matter as a function of asymmetry for normal density.

Our results indicate that temperature affects $n(k)$ in a qualitatively similar way as dynamical correlations do. The two types of correlations, however, induce quantitatively different effects and can therefore be distinguished. To separate these components, we have relied on a comparison with the FFG results, which are only affected by thermal effects. Dynamical correlations induced by the short-range NN repulsion and tensor effects, on the contrary, generate an almost momentum-independent depletion of the Fermi sea, and, complementary, lead to an occupation of high-momentum states far from the Fermi momentum.

For asymmetric systems, we find a significant change of depletion with isospin asymmetry. We identify a temperature effect for the minority protons (but not for the majority neutrons) at an asymmetry beyond $\alpha = 0.4$ at $T = 5$ MeV and normal density, due to the corresponding low density for protons. The remaining difference between the neutron and proton depletion is due to the decreased (increased) importance of tensor correlations for neutrons (protons). By considering also different operatorial clones of the Av18 interaction, like Av4', we can unambiguously demonstrate that this difference is associated with the tensor force. More importantly, the iso-depletion is independent of the chosen interaction, and therefore determined solely by phase shifts at least up to twice normal density.

We close this discussion by noting that the employed interactions appear to slightly underestimate the depletion of the experimentally determined depletion of the deep proton mean-field orbits in ^{208}Pb [17]. Nevertheless, while there remains a few % uncertainty as to the exact amount that is experimentally required, it is also clear that very different interactions, including modern ones, still lead to very similar predictions for the depletion of the nuclear Fermi sea. Such depletions can be reliably calculated with the SCGF method. When lattice QCD calculations yield unambiguous information about the short-range NN repulsion, the remaining uncertainty about the depletion of the nuclear Fermi sea will eventually be eliminated. Let us also note that the SCGF method is ideally suited to analyze two-nucleon properties in the medium and provide a theoretical interpretation of the results of two-nucleon knockout experiments [9, 10, 13].

Acknowledgments
This work has been supported by a Marie Curie Intra European Fellowship within the 7^{th} Framework programme, STFC grant ST/F012012, by the U.S. National Science Foundation under grants PHY-0652900 and PHY-0968941, by grant No. FIS2008-01661 (MEC, Spain) and grant No. 2009SGR1289 from Generalitat de Catalunya.

References

[1] Bethe H A 1971 *Annu. Rev. Nucl. Sci.* **21** 93
[2] Dickhoff W H and Van Neck D 2008 *Many-Body Theory Exposed!* 2nd ed (Singapore: World Scientific)
[3] Ishii N, Aoki S and Hatsuda T 2007 *Phys. Rev. Lett.* **99** 022001
[4] Machleidt R, Sammarruca F and Song Y 1996 *Phys. Rev. C* **53** R1483
[5] Wiringa R B, Stoks V G J and Schiavilla R 1995 *Phys. Rev. C* **51** 38
[6] Rohe D *et al.* 2004 *Phys. Rev. Lett.* **93** 182501
[7] Müther H, Polls A and Dickhoff W H 1995 *Phys. Rev. C* **51** 3040
[8] Sick I, Fantoni S, Fabrocini A and Benhar O 1994 *Phys. Lett.* **B323** 267
[9] Onderwater C J G *et al.* 1998 *Phys. Rev. Lett.* **81** 2213
[10] Starink R *et al.* 2000 *Phys. Lett.* **B474** 33
[11] Giusti C, Pacati F D, Allaart K, Geurts W J W, Dickhoff W H and Müther H 1998 *Phys. Rev. C* **57** 1691
[12] Barbieri C, Giusti C, Pacati F D and Dickhoff W H 2004 *Phys. Rev. C* **70** 014606
[13] Subedi R *et al.* 2008 *Science* **320** 1476
[14] Schiavilla R, Wiringa R B, Pieper S C and Carlson J 2007 *Phys. Rev. Lett.* **98** 132501
[15] Rios A, Polls A and Dickhoff W H 2009 *Phys. Rev. C* **79** 064308
[16] Vonderfecht B E, Dickhoff W H, Polls A and Ramos A 1991 *Phys. Rev. C* **44** R1265
[17] van Batenburg M F 2001 Ph.D. thesis University of Utrecht
[18] Lapikás L *et al.* to be submitted *Phys. Rev. Lett.*
[19] Barbieri C 2009 *Phys. Rev. Lett.* **103** 202502
[20] Mazzanti F, Polls A, Boronat J and Casulleras J 2004 *Phys. Rev. Lett.* **92** 085301
[21] Barbieri C, Van Neck D and Dickhoff W H 2007 *Phys. Rev. A* **76** 052503
[22] Fetter A L and Walecka J D 2003 *Quantum Theory of Many-Particle Systems* (NY: Dover)
[23] Rios A, Polls A, Ramos A and Müther H 2006 *Phys. Rev. C* **74** 054317
[24] Polls A, Ramos A, Ventura J, Amari S and Dickhoff W H 1994 *Phys. Rev. C* **49** 3050
[25] Frick T and Müther H 2003 *Phys. Rev. C* **68** 034310
[26] Rios A, Polls A and Vidaña I 2009 *Phys. Rev. C* **79** 025802
[27] Müther H and Dickhoff W H 2005 *Phys. Rev. C* **72** 054313
[28] Bożek P 2004 *Phys. Lett. B* **586** 239
[29] Frick T, Müther H, Rios A, Polls A and Ramos A 2005 *Phys. Rev. C* **71** 014313
[30] Gade A *et al.* 2004 *Phys. Rev. Lett.* **93** 042501
[31] Lee J *et al.* 2010 *Phys. Rev. Lett.* **104** 112701
[32] Barbieri C and Dickhoff W H 2009 *Int. J. Mod. Phys. A* **24** 2060
[33] Dickhoff W H 2010 *J. Phys. G: Nucl. Part. Phys.* **37** 064007
[34] Charity R J, Sobotka L G and Dickhoff W H 2006 *Phys. Rev. Lett.* **97** 162503
[35] Charity R J, Mueller J M, Sobotka L G and Dickhoff W H 2007 *Phys. Rev. C* **76** 044314
[36] Wiringa R B and Pieper S C 2002 *Phys. Rev. Lett.* **89** 182501